Amyloids: from molecular structure to mechanical properties

Gelderloos, C.C.

2014

document version
Publisher's PDF, also known as Version of record

Chapter 6

The polyphenol EGCG bundles and aggregates hen egg white lysozyme amyloid fibrils at neutral but not acidic pH

Based on: Corianne C. van den Akker, Tjado H.J. Morrema, Krassimir P. Velikov, Gijsje H. Koenderink (submission in preparation).

Abstract

Many diseases, including diabetes mellitus and Alzheimer's disease, are related to accumulation of aggregated (poly)peptides in tissues. These aggregates called amyloids are insoluble and up till now no adequate treatment of amyloid-related diseases is available. One of the most promising therapeutic agents is the polyphenol epi-gallocatechin-3-gallate (EGCG). It has been shown that EGCG inhibits amyloid formation for various peptides, often resulting in non-toxic oligomers. However, the mechanism behind the interactions between peptides and EGCG remains unclear. Also the knowledge on the effect of EGCG on mature amyloid fibrils is still limited. We investigated the effect of EGCG on amyloid fibrils formed from the model protein hen egg white lysozyme (HEWL) at neutral and acidic pH. We observe that at acidic pH EGCG does not affect the morphology or rigidity of HEWL amyloids fibrils. However, at neutral pH a subpopulation of thick fibrils was formed upon EGCG treatment. Electron microscopy imaging revealed that the thick fibrils formed large fibril aggregates. We show that the solution pH is an important factor in controlling the efficacy of EGCG as a therapeutic agent.

Introduction

Amyloids fibrils are protein aggregates that form from unfolded or (partially) unstructured peptides and proteins.[1] The formation of amyloids is thought to be a generic property of (poly)peptides, independent of their native fold or their amino acid sequence, although the sequence strongly influences the kinetics of amyloid formation.[2] More than 20 different human diseases are known to be related to amyloids, including type II diabetes mellitus and Alzheimer's disease.[3] These diseases have in common that a protein or peptide accumulates in an insoluble form in the affected tissue.[4] Although these macroscopic deposits of aggregates characterize protein misfolding diseases, it is thought that in many cases oligomers are substantially more cytotoxic than the fibrils.[5] Therapeutic strategies that have been proposed for treatment of amyloid-related diseases include hormones, antibodies, peptide fragments and natural antioxidants.[6] Ideally, the therapeutic agent should block the formation of oligomers and also dissociate mature fibrils into non-toxic species.[5] One of the most promising natural compounds is the polyphenol epi-gallocatechin-3-gallate (EGCG). EGCG is a catechin found in tea leaves (Figure 1a) that is thought to provide multiple health benefits since it is an antioxidant that scavenges free radicals.[6]

It has been shown that EGCG protects cells against amyloid-induced toxicity.[7-11] The reduced cytotoxicity is potentially related to the antioxidant activity of EGCG.[12] However, direct interactions of EGCG with misfolded proteins are also suggested to make a major contribution to its beneficial effects.[4] EGCG binds directly to intrinsically disordered Aβ and α-synuclein and promotes their assembly into large, non-toxic, spherical oligomers.[10] It has been shown that EGCG binds to the hydrophobic regions of several proteins, including Aβ, albumin and transthyretin.[4,13] Furthermore, it has been suggested that oxidized EGCG molecules react with free amines within the amyloid fibril, resulting in crosslinking of the fibrils.[13] EGCG inhibits fibril formation of several amyloidogenic peptides, including Aβ (Alzheimer's diseases), α-synuclein (Parkinson's disease), TTR (familial transthyretin amyloidosis) and hIAPP (type II diabetes mellitus).[9,11,14-17] Futhermore, EGCG is able to disaggregate or remodel existing amyloid fibrils (see also Chapter 4).[9,11,13,17] α-Synuclein amyloids were disaggregated into short fibrils upon incubation with EGCG for a few hours at pH=7.4.[11] Upon EGCG treatment for a few days, amorphous aggregates were formed.[11] Also α-synuclein fibrils formed amorphous aggregates that are less toxic to cells than the fibrils upon incubation with EGCG.[9] The fibril remodeling pathway is still unclear, but was shown to occur without an intermediate disassembly step.[9] No effect of EGCG on hydrophilic amyloid fibrils from the yeast prion Sup35NM was observed.[13] To investigate the effect of the hydrophilicity of the amyloid fibrils, the results were compared to amyloids fibrils with an increased

hydrophobicity obtained by mutation of two amino acids of the peptide. The hydrophobic amyloids formed a heterogeneous mix of intact fibrils and amorphous aggregates upon EGCG treatment for 24 hrs.[13]

The molecular mechanism by which EGCG interacts with amyloid fibrils and oligomers and remodels them is still unclear. Both charge-charge interactions[18] and π-π stacking interactions[14,19] of EGCG with proteins and amyloid fibrils have been reported. An important obstacle is that different studies have used different conditions for fibril assembly and incubation with EGCG. Well-controlled solution conditions are important, since the interactions between EGCG and HEWL involve noncovalent interactions that should depend on the solution pH and ionic strength.

Here we investigated the effect of EGCG on the morphology and rigidity of mature amyloid fibrils. As a model system we use amyloid fibrils formed from hen egg white lysozyme (HEWL). HEWL is a protein composed of 129 amino acid residues (Figure 1b). Its hydrophobic amino acid residues, which are likely to interact with EGCG based on prior studies of other proteins, are marked in Figure 1b. The most amyloidogenic part of HEWL is thought to be the stretch between amino acid residues 49 and 101.[20] Previously is was shown that EGCG reduces the alkali-salt mediated formation of HEWL amyloid fibrils upon incubation at pH=12.[21] Amorphous aggegates were observed upon incubation of HEWL monomer with EGCG under these using electron microscopy.[21] However, the effect of EGCG on mature HEWL fibrils is not known.

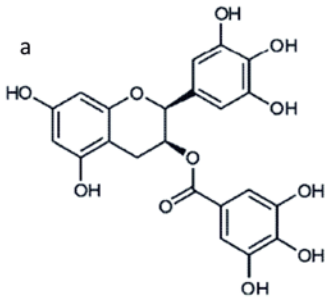

b

1 10 20 30 40
KVFGRCELAA AMKRHGLDNY RGYSLGNWVC AAKFESNFNT
41 50 60 70 80
QATNRNTDGS TDYGILQINS RWWCNDGRTP GSRNLCNIPC
81 90 100 110 120
SVNCAKKIVS SALLSSDITA DGNGMNAWVA WRNRCKGTDV
121 129
QAWIRGCRL

Figure 6.1: a) Molecular structure of EGCG. b) Amino acid sequence of HEWL. Hydrophobic amino acid residues are underlined. The most important amyloidogenic part is thought to be between amino acids residues 49 and 101.[21] V: Valine; F: Phenylalanine; C: Cysteine; L: Leucine; A: Alanine; M: Methionine; Y: Tyrosine; W: Tryptophan; P: Proline; I: Isoleucine.

Here we formed HEWL amyloids upon incubation at pH=2 and 65°C for 1 week. We compared the effect of EGCG on fibrils at the pH of formation, pH=2 and at pH=7, which is a more physiologically relevant pH level. We show that EGCG has no effect on the morphology and rigidity of fibrils at pH=2. However, at pH=7 a subpopulation of thick fibrils was formed upon incubation of preformed fibrils with EGCG in a 1:1 or 1:10 molar ratio of HEWL:EGCG. As a result, the ensemble-averaged persistence length of the fibrils increased in a dose-dependent manner at pH=7. Electron microscopy imaging revealed that the thick fibrils formed large fibril aggregates. We also show that the macroscopic viscosity of the suspensions decreases after incubation with EGCG, perhaps due to the sequestration of a fraction of the fibrils in thick fibrils and aggregates. We conclude that HEWL fibrils aggregate into thick bundles upon incubation with EGCG at pH=7, whereas at pH=2 EGCG is not able to induce any noticeable changes. Solution pH is therefore likely to be an important factor in controlling the efficacy of EGCG as a therapeutic agent.

Results and discussion

We investigated the effect of EGCG on the morphology of HEWL amyloid fibrils at pH=2 and pH=7 by imaging the fibrils after deposition and drying on a glass surface using tapping mode AFM in air. HEWL fibrils were formed by incubation at 65°C and pH=2 for 1 week. To remove non-aggregated material and small oligomers, the samples were filtered with 100kDa molecular weight cut-off filters. Long, thin fibrils with a length up to several micrometers were formed (Figure 6.2a-b). The fibrils were incubated with EGCG in a molar ratio of either 1:1 or 1:10 (HEWL:EGCG), for either 2 or 24 hrs, all at room temperature. At acidic pH (pH=2), we observed no visible effect of EGCG on the morphology of the fibrils based on AFM images (Figure 6.2c-f).

To test the effect of EGCG at neutral pH (pH=7), fibrils were transferred to water at pH=7 by filtration over 100 kDa molecular weight cut-off filters and washing with MilliQ water. The transfer process did not visibly change the morphology of the fibrils based on AFM images (Figure 6.3a-b). Note that in some AFM images of control samples, both at pH=2 and pH=7, short fragments were observed (Figure 6.3a). We do not know the origin of the variability between different images. Incubation with EGCG in a 1:1 HEWL:EGCG molar ratio at pH=7 for either 2 or 24 hrs did not result in a visible change fibril morphology (Figure 6.3c-d). However, upon incubation in a 1:10 HEWL:EGCG molar ratio, we observed a population of thick fibrils (Figure 6.3e-f).

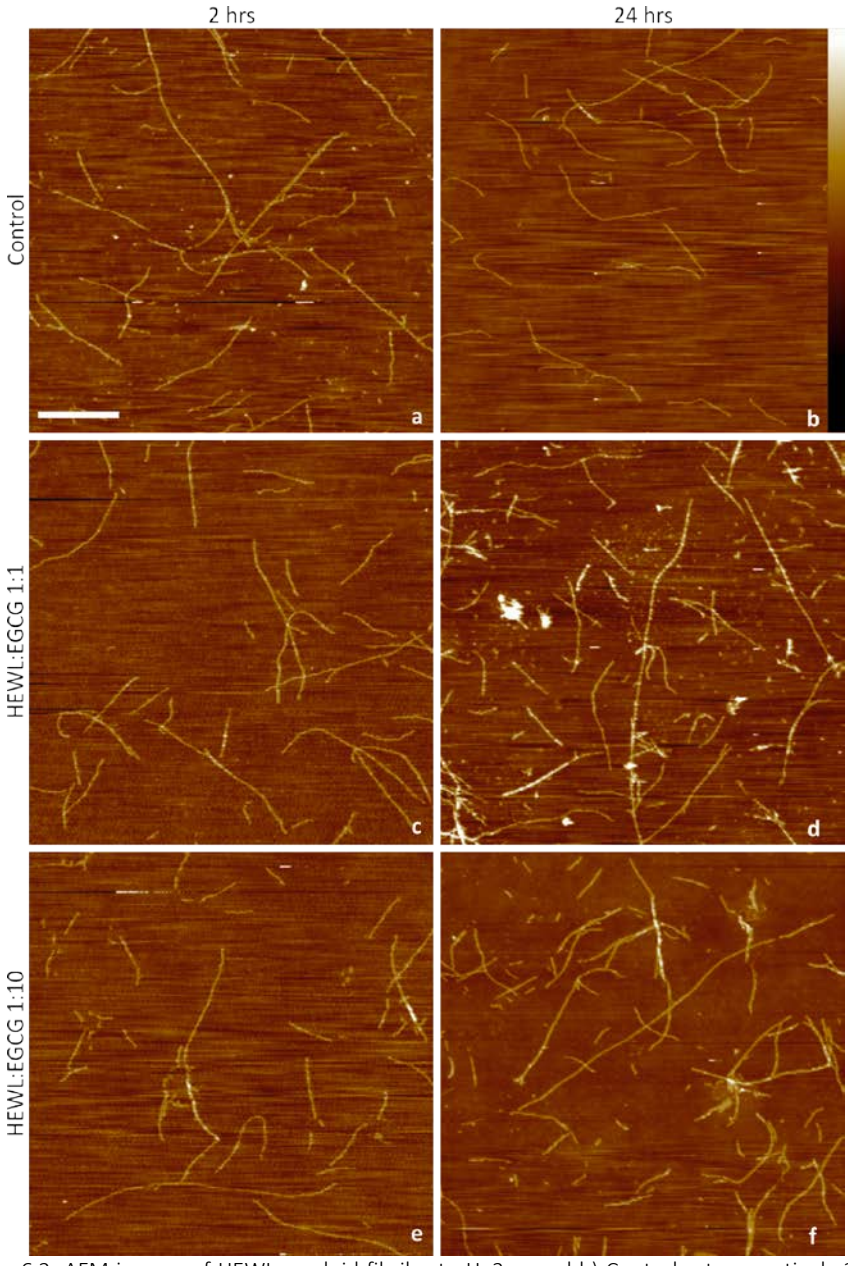

Figure 6.2: AFM images of HEWL amyloid fibrils at pH=2. a and b) Controls at respectively 2 and 24 hrs; c and d) Incubation with EGCG in 1:1 molar ratio HEWL:EGCG for 2 and 24 hrs ; e and f) Incubation with EGCG in 1:10 molar ratio HEWL:EGCG for 2 and 24 hours. Scale is the same for all images, scale bar is 2 µm, AFM height bar (right hand side of panel (b)) is 20 nm.

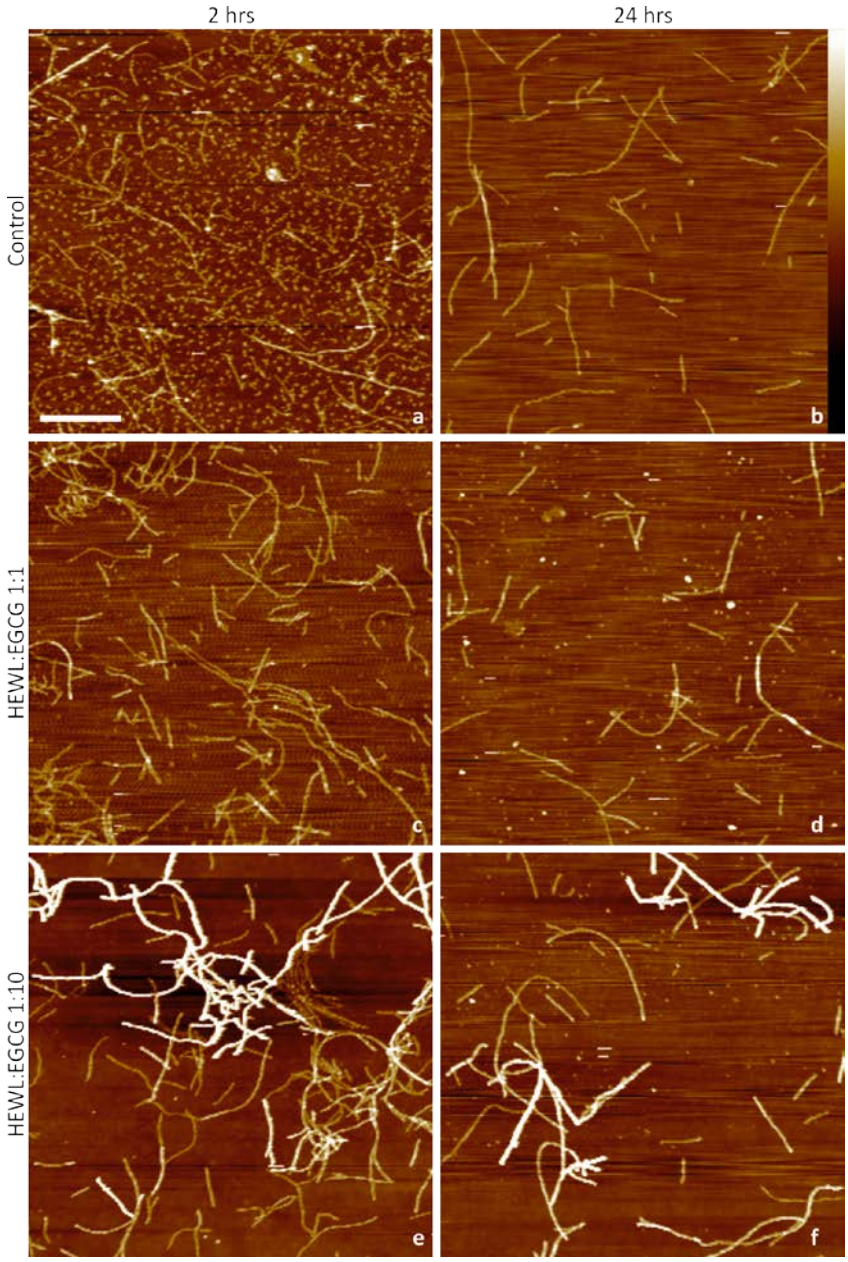

Figure 6.3: AFM images of HEWL amyloid fibrils at pH=7. a and b) Controls at respectively 2 and 24 hrs; c and d) Incubation with EGCG in 1:1 molar ratio HEWL:EGCG for 2 and 24 hrs ; e and f) Incubation with EGCG in 1:10 molar ratio HEWL:EGCG for 2 and 24 hours. Scale is the same for all images, scale bar is 2 µm, AFM height bar (right hand side of panel (b)) is 20 nm.

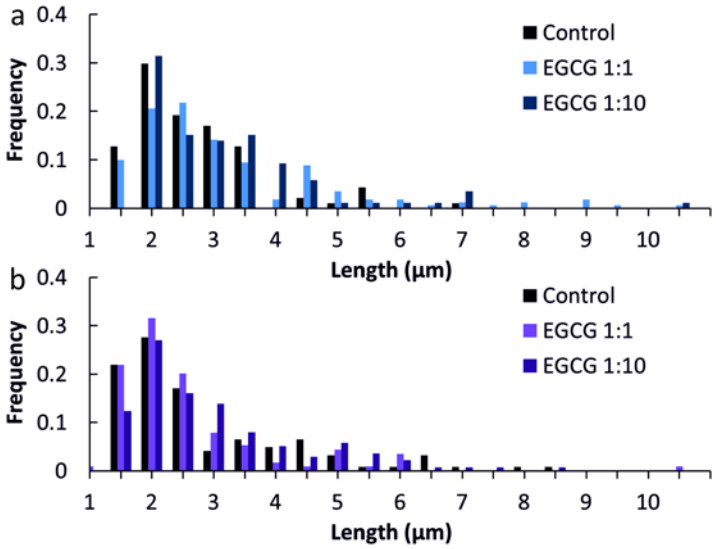

Figure 6.4: Length distributions of fibrils incubated for 24 hrs with EGCG in a 1:1 or 1:10 molar ratio HEWL:EGCG. a) Fibrils at pH=2. b) Fibrils at pH=7.

To investigate the effect of EGCG on the morphology of the fibrils in more quantitative detail, we measured the contour lengths and diameters of the fibrils by image analysis. Both at pH=2 and pH=7, the fibrils show a broad length distribution, with an average length of approximately 2 µm (Figure 6.4 and Table 6.1). The contour length did not change upon incubation with EGCG at either pH condition. For fibrils at pH=2, the average diameter was 3.7 ± 1.1 nm and remained unchanged upon incubation with EGCG (Figure 6.5a and Table 6.1). The fibrils at pH=7 had a similar diameter distribution with an average of 4.6 ± 1.4 nm (Figure 6.5b and Table 6.1). Upon incubation with EGCG, the diameter distribution of the fibrils at pH=7 shifts to higher values. The average diameter upon incubation with EGCG in a 1:1 molar ratio for 24 hrs increases to 5.6 ± 1.2 nm. Upon incubation with EGCG in a 1:10 molar ratio for 24 hrs, the average diameter increases even more, to 7.7 ± 1.4 nm. Although there were still thin fibrils present, a broad distribution of diameters was observed, with the thickest fibrils having diameters larger than 15 nm, indicating the formation of a new population of fibrils.

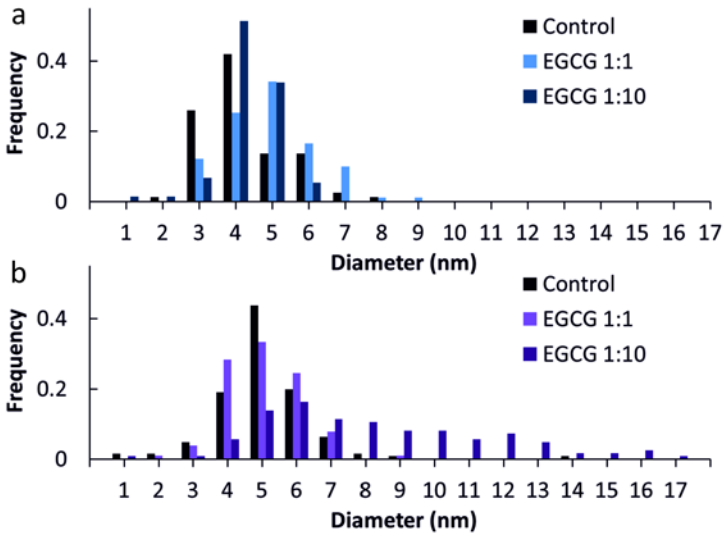

Figure 6.5: Diameter distributions of fibrils incubated for 24 hrs with EGCG in a 1:1 or 1:10 molar ratio HEWL:EGCG. a) Fibrils at pH=2. b) Fibrils at pH=7.

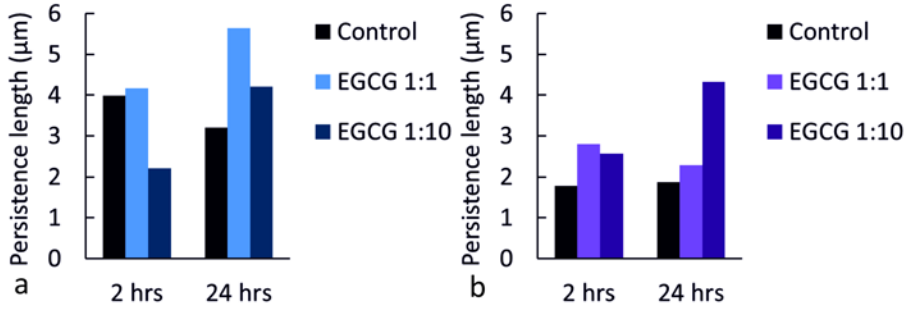

Figure 6.6: Persistence length of HEWL fibrils incubated for 2 or 24 hrs with no EGCG or with EGCG in a 1:1 or 1:10 HEWL:EGCG molar ratio at a) pH=2; b) pH=7.

Since the presence of the thick fibrils was the most striking change upon incubation with EGCG, we analyzed the surface topography of these thick fibrils more closely. The thick fibrils are composed of thin fibrils twisted together with a periodicity of approximately 120 nm (Figure 6.7b). We also observed a population of twisted fibrils in control samples, but these had a smaller diameter of around 6 nm and a smaller periodicity of approximately 90 nm. Previous AFM studies showed the presence of flat, ribbon-like fibrils of HEWL composed of up to 16 protofilaments upon incubation at pH=2 and 90°C.[22] However, these fibrils are clearly different in size and morphology than the twisted fibrils we observe in the presence of EGCG.

Table 6.1: Overview of the effect of incubation with EGCG in 1:1 or 1:10 molar ratio HEWL:EGCG on average contour length, diameter and persistence length of fibrils at pH=2 or pH=7. Average contour lengths and diameters are based on more than 86 fibrils per condition. For persistence length calculations only fibrils longer than 2 µm were used, the number of analyzed fibrils is indicated.

pH	EGCG	Incubation time (hrs)	Contour length (µm)	Diameter (nm)	Persistence length (µm)	# fibrils analyzed for persistence length
2	No EGCG	2			4.0	53
		24	1.9 ± 1.1	3.7 ± 1.1	3.2	50
2	1:1	2			4.2	38
		24	2.5 ± 1.7	4.4 ± 1.2	5.6	46
2	1:10	2			2.2	54
		24	2.5 ± 1.5	3.8 ± 0.9	4.2	34
7	No EGCG	2			1.8	65
		24	2.0 ± 1.4	4.6 ± 1.4	1.9	68
7	1:1	2			2.8	56
		24	1.9 ± 1.4	5.6 ± 1.2	2.3	66
7	1:10	2			2.6	53
		24	2.3 ± 1.4	7.7 ± 3.2	4.3	44

To investigate whether the change in diameter upon incubation with EGCG affects the bending rigidity of the fibrils, we determined the persistence length based on AFM images of a large ensemble of fibrils. Fibrils were imaged on glass, because in a parallel study we found evidence that the HEWL fibrils can equilibrate their conformations before adsorbing onto the surface (see also Chapter 7). This assumption is qualitatively validated by the absence of looped conformations. For all samples, only fibrils with a length over 2 µm were used in the analysis, to ensure that the transverse undulations of the fibrils are detectable by AFM. We analyzed the average mean-square angle $\langle \Theta^2 \rangle$ of dried fibrils as a function of the fibril contour length. The dependence was fitted by a theoretical model for semiflexible polymers, according to which $\langle \Theta^2(s) \rangle_{2D} = C/L_p$, where *s* is the segment length, *C* is the contour length and L_p is the persistence length[23]. For fibrils at pH=2, we obtained an average persistence length of 3.2 µm, similar to our observations in Chapter 7 and slightly higher than values reported in literature for HEWL amyloid fibrils formed under similar conditions[24]. Although we did not observe an effect of EGCG on the diameter at pH=2, the persistence length did appear to change slightly upon incubation in a 1:10 molar ratio for 2 hrs (2.2 µm) but not after incubation for 24 hrs (4.2 µm) (Figure 6.6a and Table 6.1).

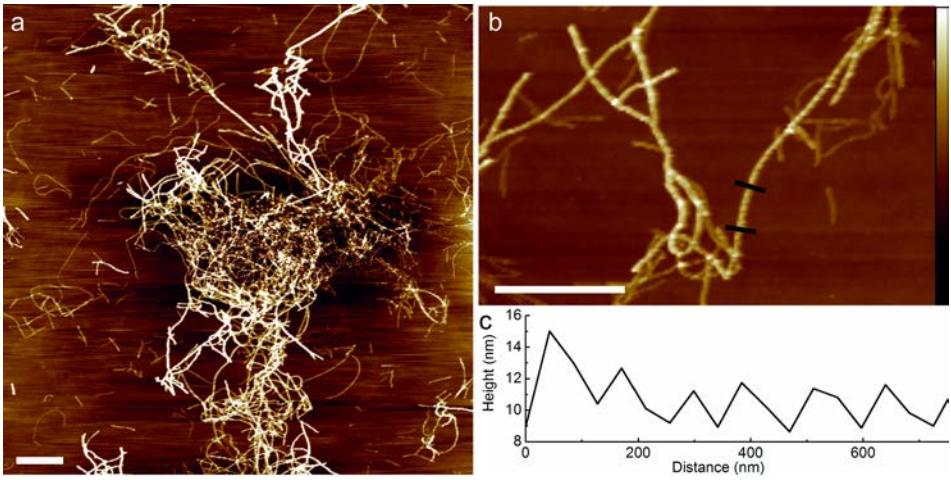

Figure 6.7: a) AFM image of fibrils incubated with EGCG at a 1:10 molar ratio EGCG:HEWL at pH=7 for 2 hrs. Scale bar is 2 µm, height bar (shown in (b)) is 20 nm. b) Zoom-in of thick fibrils formed upon incubation with EGCG at a 1:10 molar ratio for 2 hrs. Scale bar is 2 µm, height bar is 20 nm. c) Periodicity in height of the fibril section delimited by the black lines of the fibril in (b). The height fluctuations show a periodicity of approximately 120 nm. Thin fibrils in the same image do not show a periodicity.

The average persistence length of fibrils at pH=7 is 1.8 µm, approximately twice as low as at pH=2 (Figure 6.6b and Table 6.1). It is possible that the structure of the fibrils changes upon the change of pH, resulting in less rigid fibrils. Additional measurements of the persistence length in solution by time-lapse fluorescence imaging could help to settle this issue. Upon incubation with EGCG in a 1:1 molar ratio, the persistence length increases slightly compared to the control case, both for incubation times of 2 and 24 hrs. Incubation with EGCG in a 1:10 molar ratio results in a pronounced increase of the persistence length compared to the control case. After 2 hrs, the persistence length is increased from 1.8 µm to 2.6 µm, and after 24 hrs it is increased to 4.3 µm. These increases likely reflect the presence of the population of thick fibrils that was observed upon incubation with EGCG in a 1:10 molar ratio. It would be interesting to determine the persistence length of the population of thick fibrils separately, and compare this to the persistence length of the thin fibrils. However, it is complicated to compare these two populations using the method based on AFM images, because a large proportion of the thick fibrils forms aggregates. In future, the persistence length of this thick fibril population could be determined by the analysis of the undulations of freely fluctuating fibrils in water, as described in Chapter 7.

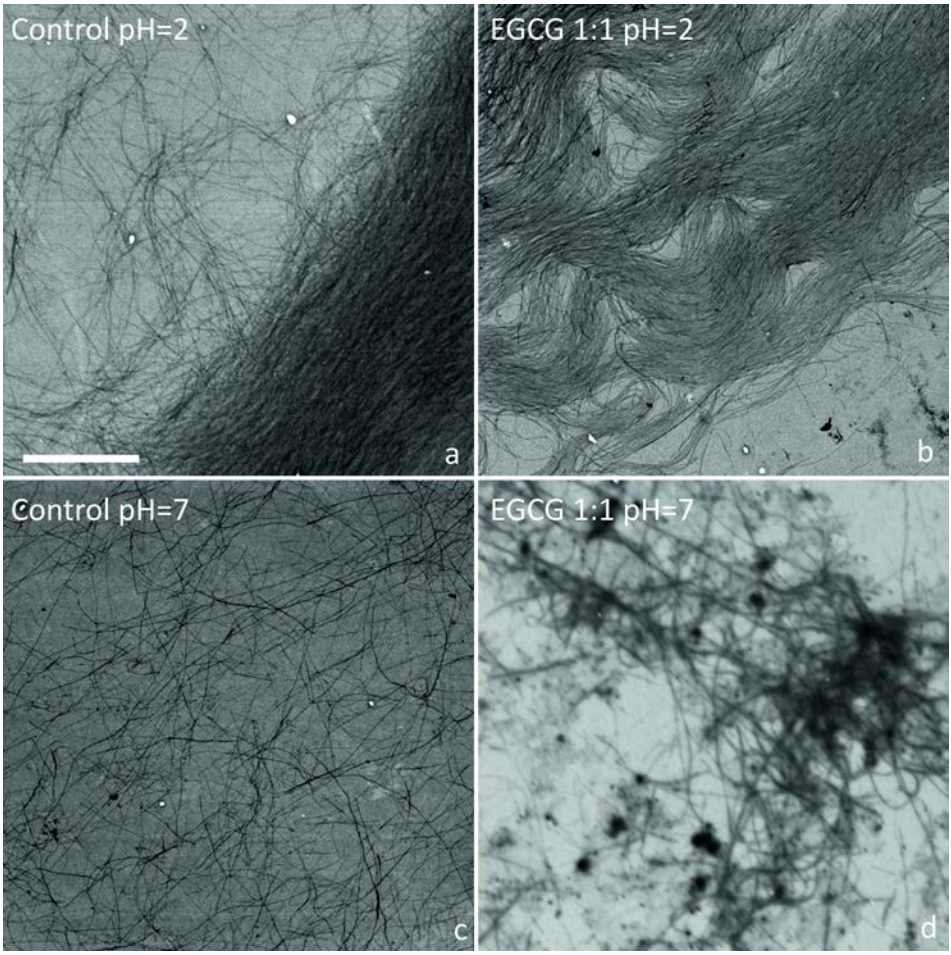

Figure 6.8: Scanning transmission electron microscopy (STEM) images of HEWL amyloid fibrils at a and b) pH=2 or c and d) pH=7. Fibrils in b and d were incubated with EGCG in a HEWL:EGCG 1:1 molar ratio for 24 hrs. At pH=2, no effect of EGCG is observed, while at pH=7 thick fibrils forming fibril aggregates (arrow 1 in (d)) and dense aggregates (arrow 2 in (d)) are observed.

AFM imaging at pH 7 revealed a few large aggregates that were mainly composed of thick fibrils (Figure 6.7a). These aggregates were not observed in any of the samples (with or without EGCG) at pH=2 or in the control samples at pH=7. The aggregation suggests that the surface of the thick fibrils may be changed upon incubation with EGCG, resulting in stronger interactions between the fibrils. Because with AFM only relatively small sample areas can be imaged, we investigated the formation of the large fibril aggregates more extensively using scanning transmission electron microscopy (STEM). Figure 6.8a shows a STEM image of control fibrils at pH=2. The fibrils are

variously distributed on the surface, being more randomly distributed in some places and bundled and aligned in other places. After incubation with EGCG in a 1:1 molar ratio for 24 hrs, the samples look similar in STEM, and no aggregates were observed (Figure 6.8b). At pH=7, the control fibrils formed a fine, isotropic network (Figure 6.8c). In the control sample, no aggregates were observed. However, upon incubation with EGCG in a 1:1 molar ratio for 24 hrs, the morphology of the network changed. Large fibril aggregates were observed (Figure 6.8d), mainly containing thick fibrils. The formation of fibril aggregates at pH=7 was observed previously for HEWL fibrils incubated with EGCG in a molar ratio of 5:1 (HEWL:EGCG) for 2 hrs.[25] However, in that study the fibril suspension was not filtered before incubation with EGCG, which makes it difficult to conclude whether the aggregates were formed from monomers, oligomers or mature fibrils. Besides the fibril aggregates, we observed also dense clusters in the STEM images of fibrils incubated with EGCG at pH=7. Similar clusters were also observed in STEM images of fibrils formed from β-lg without the presence of EGCG.

The observations that the morphology and persistence length of the fibrils changes and the fibrils form aggregates upon incubation with EGCG at pH=7 raises the question whether it is possible to observe a macroscopic change in network rheology. To test this, we measured the shear-rate dependent viscosity of the fibril suspensions (Figure 6.9a and b). The suspensions all exhibited strong shear-thinning behavior over the large range of shear rates that we measured (from 10^{3} to 10^{-3} s^{-1}), similar to suspensions of amyloid fibril suspensions formed from β-lactoglobulin (Chapter 8). Fibril suspensions at pH=2 incubated with EGCG in a 1:1 or 1:10 molar ratio did not show changes in viscosity. The fibril suspension at pH=7 showed a similar shear rate dependent viscosity as the control sample at pH=2. Upon incubation with EGCG in a 1:1 molar ratio, no changes in viscosity were observed. However, upon incubation in a 1:10 molar ratio, the low-shear viscosity decreased while the high-shear viscosity was unchanged. To compare the results of fibrils at pH=2 and pH=7, we plotted the viscosities measured at low (10^{-3} s^{-1}) and high (10^{3} s^{-1}) shear rate for all different conditions in Figure 6.9c and d. The low-shear viscosity decreases slightly for fibrils incubated with EGCG in a 1:10 molar ratio for 24 hrs, while the high-shear viscosity remains constant. This observation suggests that the direct interactions between fibrils, which contribute to the low-shear but not the high-shear viscosity, may be subtly changed. In principle, adhesive interactions would be expected to increase the low-shear viscosity. However, fibril aggregation and the resulting sample inhomogeneity may reduce the viscosity. Using rheology alone we cannot separate these effects.

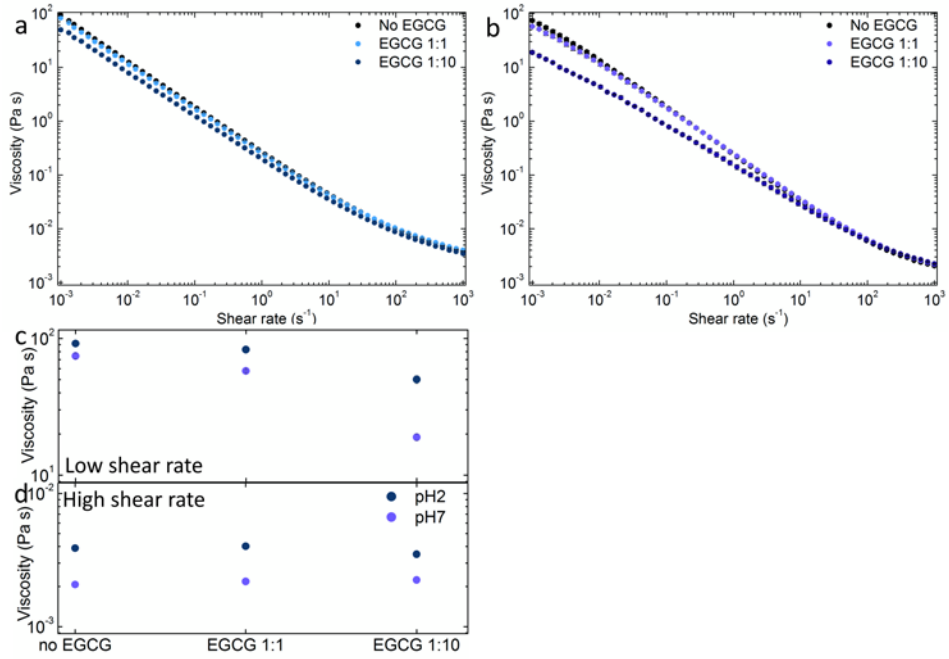

Figure 6.9: Shear rate dependent viscosity of suspensions of HEWL fibrils at a) pH=2 and b) pH=7, incubated without or with EGCG in a 1:1 or 1:10 HEWL:EGCG molar ratio for 24 hrs. c and d) Viscosities measured at low (10^{-3} s^{-1}) and high (10^{3} s^{-1}) shear rate, respectively, for fibril suspensions at pH=2 and pH=7. Error bars are smaller than the size of the symbols.

Several studies reported the formation of large amorphous aggregates upon incubation of mature amyloid fibrils with EGCG for a variety of proteins and peptides.[9,13,25] These results are reminiscent of our observation of the formation of large fibril aggregates upon incubation of HEWL fibrils with EGCG at pH=7. We show that the aggregates are mainly composed of thick fibrils. The thick fibrils are presumably bundles of amyloid fibrils. This is in agreement with a previous study of α-synuclein showing that EGCG treatment did not reverse the amyloid formation process, but directly bundled fibrils into thick fibrils and aggregates[9]. It was shown using fluorescence microscopy that upon incubation of red and green fluorescently labeled fibrils with EGCG, aggregates predominantly labeled by either the green or the red fluorophores were formed. It was proposed that the aggregates are less toxic to cells than the fibrils.[9] It has been shown that EGCG can interact with proteins and amyloid fibrils via charge-charge interactions[18] and π-π stacking interactions[14,19]. At pH=2, charge-charge interactions are unlikely, because both the amino acids and EGCG are protonated under acidic conditions. This may explain why we do not see any effect of EGCG on amyloid fibrils at pH=2, while there is a strong effect observed at pH=7.

Conclusions

We investigated the effect of EGCG on the morphology and bending rigidity of HEWL amyloid fibrils at pH=2 and pH=7. At pH=2, no effect of EGCG was observed, even after incubation for 24 hrs with a tenfold molar excess of EGCG. However, incubation with EGCG at pH=7 resulted in the formation of a subpopulation of thick fibrils. The thick fibrils with diameters up to 17 nm formed large fibril aggregates. At a molar ratio of 1:10 HEWL:EGCG, these thick fibrils were already observed after 2 hrs. No effect of EGCG on the contour length was observed, but the average diameter of HEWL fibrils increased from 4.6 ± 1.4 nm to 7.7 ± 3.2 nm in a dose-dependent manner. Also the average persistence length increased upon incubation with EGCG in a 1:10 molar ratio, from 1.9 µm to 4.3 µm upon incubation for 24 hrs. Large fibril aggregates and thick fibrils were also observed in STEM images of fibrils incubated with EGCG at pH=7, both upon incubation in a 1:1 molar ratio for 24 hrs and in a 1:10 molar ratio for 2 hrs. The low-shear viscosity decreased slightly upon incubation with EGCG in a 1:10 molar ratio for 24 hrs, likely due to the formation of thick fibril bundles and fibril aggregates. It is likely that charge-charge interactions between EGCG and the fibrils play an important role in the aggregation and bundling of fibrils since no effect of EGCG was observed at pH=2, when the amino acid residues are protonated, while EGCG was able to bundle amyloid fibrils at pH=7. More detailed follow-up studies of the effects of EGCG on the molecular packing structure of the fibrils and surface composition are needed to clarify how EGCG affects fibril morphology and organization. Such studies are a prerequisite to understand how EGCG may act as a potential therapeutic agent to combat amyloid-related diseases.

Materials and methods

Amyloid formation and incubation with EGCG. Hen egg white lysozyme powder (HEWL, Sigma Aldrich cat # 62970) was dissolved in an aqueous HCl solution (pH=2.0) and the pH was immediately adjusted to pH=2.0. HEWL was dissolved by stirring the solution for 1 hr at 4°C. To remove traces of electrolytes, the solution was dialyzed against a HCl solution (pH=2.0) at 4°C using a slide-a-lyzer (Thermo Scientific cat. #87732) with a molecular weight cut-off (MWCO) of 10 kDa. Aggregates were removed by filtration with a 0.1 µm filter (Sigma Aldrich #F7523). The protein concentration was calculated based on measurements of light absorption at 280 nm with a Nanodrop spectrophotometer (Thermo Scientific), using an extinction coefficient of 37,752 $M^{-1} cm^{-1}$.[26] Amyloid fibrils were formed by incubation of 30 mL of the monomer solution at a concentration of 1 mM in a polypropylene tube in an oven at 65°C for 7 days, while the solution was stirred using a magnetic stirrer. After 7 days, samples were quenched on ice water and fibrils were separated from small aggregates and monomers by filtration

using centrifugal filters (Amicon, Millipore cat.#UFC910024) with a MWCO of 100 kDa. Prewashed filters were centrifuged at 1000 g for 30 min and samples were subsequently washed 3 times with a HCl solution (pH=2.0) by repeating the centrifugation. For experiments at pH=7, the washing steps were performed with water instead of a HCl solution. No buffer was used, because it has been observed that fibrils aggregate in the presence of salts. EGCG powder (Sigma Aldrich cat # E4143) was dissolved in MilliQ or a HCl solution at pH=2. EGCG solutions were prepared freshly before each experiment to prevent degradation[27]. Amyloid fibrils were incubated with EGCG in a 1:1 or 1:10 molar ratio HEWL:EGCG for 2 or 24 hrs at room temperature in dark to prevent photodegradation[28].

Atomic Force Microscopy (AFM). Filtered fibril suspensions were diluted to protein concentrations of approximately 1 µM and 15 µL of the suspension was incubated on glass cover slips cleaned with isopropanol. After 3 minutes, the slides were washed with HCl solution at pH=2.0, and dried in air. Atomic force microscopy imaging was performed on a Dimension 3100 Scanning Probe Microscope (Bruker) using silicon cantilevers (TESPA, force constant 42 N/m, Bruker). All images were flattened using Nanoscope 6.14 software. The fibrils were manually tracked using the Simple Neurite Tracer plugin in Fiji.[29]

Scanning transmission Electron Microscopy (STEM). Fibril suspensions were diluted to peptide concentrations of 10 µM. Samples for STEM were prepared by incubation of 1 µL of the fibril suspension on a carbon coated copper grid with 300 µm mesh size (TED PELLA INC) for 5 min. Excess liquid was removed, the samples were washed with MilliQ water and dried in air. Scanning transmission electron microscopy was performed on a Verios 460 microscope (FEI) operating at 5 kV. Images were obtained in bright field. The image contrast was enhanced using ImageJ software.

Rheology. A stress-controlled rheometer (Physica MCR 501, Anton Paar) with steel cone (30 mm diameter, 1° angle) and plate thermostatted with a Peltier plate were used for rheometry. Evaporation was reduced by closing off the geometry with a cover during measurements. The nonlinear rheology was determined by measurement of the viscosity as a function of shear rate, with shear rates ramping down from 10^{3} to 10^{-3} s^{-1}. All measurements were performed at T=21°C. All experiments were performed at least twice, error bars show the standard deviation.

Acknowledgment

The authors thank Norbert Mücke (DKFZ Heidelberg, Germany) for providing software for persistence length calculations and Andries Lof (FOM Institute AMOLF, The Netherlands) for assistance with STEM imaging. This work is part of the Industrial Partnership Programme (IPP) Bio(-Related) Materials (BRM) of the Stichting voor Fundamenteel Onderzoek der Materie (FOM), which is financially supported by the Nederlandse Organisatie voor Wetenschappelijk Onderzoek (NWO). The IPP BRM is co-financed by the Top Institute Food and Nutrition and the Dutch Polymer Institute.

References

(1) Dobson, C. M. *Nature* 2003, *426*, 884.
(2) Stefani, M.; Dobson, C. M. *Journal of Molecular Medicine* 2003, *81*, 678.
(3) Chiti, F.; Dobson, C. M. *Annual Review of Biochemistry* 2006, *75*, 333.
(4) Bieschke, J. *Neurotherapeutics* 2013, *10*, 429.
(5) Attar, A.; Rahimi, F.; Bitan, G. *Translational Neuroscience* 2013, *4*, 385.
(6) He, J.; Xing, Y. F.; Huang, B.; Zhang, Y. Z.; Zeng, C. M. *Journal of Agricultural and Food Chemistry* 2009, *57*, 11391.
(7) Jayasena, T.; Poljak, A.; Smythe, G.; Braidy, N.; Münch, G.; Sachdev, P. *Ageing Research Reviews* 2013, *12*, 867.
(8) Bieschke, J.; Russ, J.; Friedrich, R. P.; Ehrnhoefer, D. E.; Wobst, H.; Neugebauer, K.; Wanker, E. E. *Proceedings of the National Academy of Sciences of the United States of America* 2010, *107*, 7710.
(9) Lopez del Amo, J. M.; Fink, U.; Dasari, M.; Grelle, G.; Wanker, E. E.; Bieschke, J.; Reif, B. *Journal of Molecular Biology* 2012, *421*, 517.
(10) Meng, F.; Abedini, A.; Plesner, A.; Verchere, C. B.; Raleigh, D. P. *Biochemistry* 2010, *49*, 8127.
(11) Norton, R. S.; Chandrashekaran, I. R.; Adda, C. G.; MacRaild, C. A.; Anders, R. F. *Biochemistry* 2010, *49*, 5899.
(12) Ferreira, N.; Saraiva, M. J.; Almeida, M. R. *Febs Letters* 2011, *585*, 2424.
(13) Engel, M. F. M.; vandenAkker, C. C.; Schleeger, M.; Velikov, K. P.; Koenderink, G. H.; Bonn, M. *Journal of the American Chemical Society* 2012.
(14) Palhano, F. L.; Lee, J.; Grimster, N. P.; Kelly, J. W. *Journal of the American Chemical Society* 2013, *135*, 7503.
(15) Choi, Y. T.; Jung, C. H.; Lee, S. R.; Bae, J. H.; Baek, W. K.; Suh, M. H.; Park, J.; Park, C. W.; Suh, S. I. *Life Sciences* 2001, *70*, 603.
(16) Li, M. H.; Jang, J. H.; Sun, B. X.; Surh, Y. J. In *Signal Transduction Pathways, Chromatin Structure, and Gene Expression Mechanisms as Therapeutic Targets*; Diederich, M., Ed. 2004; Vol. 1030, p 317.
(17) Ehrnhoefer, D. E.; Bieschke, J.; Boeddrich, A.; Herbst, M.; Masino, L.; Lurz, R.; Engemann, S.; Pastore, A.; Wanker, E. E. *Nature Structural & Molecular Biology* 2008, *15*, 558.
(18) Kim, H.-S.; Quon, M. J.; Kim, J.-a. *Redox Biology* 2014, *2*, 187.
(19) Ozdal, T.; Capanoglu, E.; Altay, F. *Food Research International* 2013, *51*, 954.
(20) Porat, Y.; Abramowitz, A.; Gazit, E. *Chemical Biology & Drug Design* 2006, *67*, 27.

(21) Frare, E.; Polverino de Laureto, P.; Zurdo, J.; Dobson, C. M.; Fontana, A. *Journal of Molecular Biology* **2004**, *340*, 1153.
(22) Ghosh, S.; Pandey, N. K.; Dasgupta, S. *International Journal of Biological Macromolecules* **2013**, *54*, 90.
(23) Lara, C. c.; Adamcik, J.; Jordens, S.; Mezzenga, R. *Biomacromolecules* **2011**, *12*, 1868.
(24) Mücke, N.; Kreplak, L.; Kirmse, R.; Wedig, T.; Herrmann, H.; Aebi, U.; Langowski, J. *Journal of Molecular Biology* **2004**, *335*, 1241.
(25) Lara, C.; Usov, I.; Adamcik, J.; Mezzenga, R. *Physical Review Letters* **2011**, *107*, 238101.
(26) Mishra, R.; Sorgjerd, K.; Nystrom, S.; Nordigarden, A.; Yu, Y. C.; Hammarstrom, P. *Journal of Molecular Biology* **2007**, *366*, 1029.
(27) Sang, S. M.; Lee, M. J.; Hou, Z.; Ho, C. T.; Yang, C. S. *Journal of Agricultural and Food Chemistry* **2005**, *53*, 9478.
(28) Bianchi, A.; Marchetti, N.; Scalia, S. *Journal of Pharmaceutical and Biomedical Analysis* **2011**, *56*, 692.
(29) Longair, M. H.; Baker, D. A.; Armstrong, J. D. *Bioinformatics* **2011**.